

Identifying Adversarially Attackable and Robust Samples

Vyas Raina
 ALTA Institute, University of Cambridge
 vr313@cam.ac.uk

Mark Gales
 ALTA Institute, University of Cambridge
 m.j.gales@cam.ac.uk

Abstract

Adversarial attacks insert small, imperceptible perturbations to input samples that cause large, undesired changes to the output of deep learning models. Despite extensive research on generating adversarial attacks and building defense systems, there has been limited research on understanding adversarial attacks from an input-data perspective. This work introduces the notion of sample attackability, where we aim to identify samples that are most susceptible to adversarial attacks (attackable samples) and conversely also identify the least susceptible samples (robust samples). We propose a deep-learning-based method to detect the adversarially attackable and robust samples in an unseen dataset for an unseen target model. Experiments on standard image classification datasets enables us to assess the portability of the deep attackability detector across a range of architectures. We find that the deep attackability detector performs better than simple model uncertainty-based measures for identifying the attackable/robust samples. This suggests that uncertainty is an inadequate proxy for measuring sample distance to a decision boundary. In addition to better understanding adversarial attack theory, it is found that the ability to identify the adversarially attackable and robust samples has implications for improving the efficiency of sample-selection tasks, e.g. active learning in augmentation for adversarial training¹.

1. Introduction

Deep learning models have achieved remarkable success across a wide range of tasks and domains, including image classification [10] and natural language processing [15]. However, these models are also susceptible to adversarial attacks [8], where small, imperceptible perturbations to the input can cause large, undesired changes to the output of the model [13, 28, 38]. Extensive research has been conducted on generating adversarial attacks and building defense systems [2, 3], such as detection [11, 24, 29–31] or ad-

versarial training [1, 22, 23]. However, little or no work has sought to understand adversarial attacks from an input-data perspective. In particular, it is unclear why some samples are more susceptible to attacks than others. Some samples may require a much smaller perturbation for a successful attack (*attackable samples*), while others may be less susceptible to imperceptible attacks and require much larger perturbations (*robust samples*). Determining the *attackability* of samples can have important implications for various tasks, such as active learning [25, 33] and adversarial training [23]. In the field of active learning, adversarial perturbation sizes can be used by the acquisition function to select the most useful/uncertain samples for training [4, 26]. Similarly, adversarial training can be made more efficient by augmenting with adversarial examples for only the most attackable samples to avoid unnecessarily scaling training times, i.e. a variant of weighted adversarial training [12].

This work defines the notion of sample attackability: the smallest perturbation size required to change a sample’s output prediction. To determine if a particular sample is *attackable* or *robust*, we use the *imperceptibility* threshold in the definition of an adversarial attack. In automated adversarial attack settings, a proxy function is often used to measure human perception [27] and thus there can be a range of acceptable threshold’s for the imperceptibility boundary, as per the proxy measure. In this work, If a sample’s minimum perturbation size is within a *strict* threshold of imperceptibility, then the sample is considered an adversarially attackable sample. In converse, a sample with a perturbation size greater than a much more generous threshold for *imperceptibility* is termed as robust. Further, this work proposes a simple deep-learning based method to detect the attackable and robust samples, agnostic to a specific model’s realisation or architecture. The attackability detector is evaluated on an unseen dataset, for an unseen target model. Further, the attackability detector is evaluated with an unmatched adversarial attack method; i.e. the detector is trained using perturbation sizes defined by the simple Finite Gradient Sign Method (FGSM) attack [8], but evaluated on sample perturbation sizes calculated using the more powerful Project Gradient Descent (PGD)

¹Code available at: https://github.com/rainavyas/img_attackability

attack method [20]. The deep-learning based attackability detector is also compared to alternative uncertainty [5] based detectors.

Contributions of this work can be summarised as follows:

- Formal definition for the notion of adversarially attackable and robust samples.
- Proposal of a simple and effective deep-learning method to identify attackable and robust samples, agnostic of model design, as well as being portable across attack methods.
- Application of the sample attackability detector in improving the efficiency of adversarial training.

2. Related Works

Understanding adversarial samples: A range of hypotheses exist for explaining the existence of adversarial examples. These explanations are either model/architecture-orientated or from an input data perspective. For understanding sample *attackability*, it is more useful to consider explanations from the data perspective. Initial explanations [9, 34] argued that adversarial examples lie in large and continuous *pockets* of the data manifold (low-probability space), which can be easily accessed. Conversely, it is also hypothesized [35] that adversarial examples simply lie in low variance directions of the data, but this explanation is often challenged [14]. Similarly, many pieces of work [6, 19, 21, 32] argue that adversarial examples lie orthogonal to the data manifold and can so can easily be reached with small perturbations. It can also be argued [7] that adversarial examples are a simple consequence of intricate and high-dimensional data manifolds. Nevertheless, these hypotheses do not offer an explicit explanation or method for identifying individual sample-level susceptibility to adversarial attacks.

Use of adversarial perturbations: In the field of active learning [25, 33], methods have been proposed to exploit adversarial attacks to determine the minimum perturbation size for each sample in a dataset and then the samples are ranked by this perturbation size. The perturbation size is viewed as a proxy for distance to a model’s decision boundary and thus an acquisition function selects the samples with the smallest perturbations for training the model. However, perturbation sizes are very specific to the model being trained, as opposed to contributing to the overall measure of the *attackability* of a sample, agnostic of the model and adversarial attack method. This work seeks to explicitly identify the attackable and robust samples in an unseen dataset independent of a specific model realisation

or architecture.

Weighted Adversarial Training Knowledge of sample attackability can be applied to the field of adversarial training. Adversarial training [23] is a popular method to enhance the robustness of systems, where a system is trained on adversarial examples. However, certain adversarial examples can be more *useful* than others and hence certain research attempts have explored reweighing of adversarial examples during training. Once adversarial example have been generated, the adversarial training loss function can be adapted to give greater importance to capture an adversarial example’s class margin [12]. Alternatively, adversarial examples can be re-weighted using the model confidence associated with each example, where it is assumed that the least confident adversarial examples are best for adversarial training [37]. However, as opposed to considering the full set of generated adversarial examples, it is more useful to determine which original/non-adversarial samples it is worth using to generate an adversarial example for the purpose of adversarial training. An effective proposed approach [16] exploits model uncertainty (such as entropy) associated with each original sample and then adversarial examples need to be generated only for the least certain samples. In the domain of natural language processing, it has been shown that an online meta-learning algorithm can also be used to learn weights for the original samples [36]. In contrast to the above methods, this work is the first to use a deep learning approach to predict perturbation sizes for the original/non-adversarial samples, independent of the attack and target model and thus offer an alternative and demonstrably more effective method for weighted adversarial training.

3. Adversarial Attacks

An untargeted adversarial attack is successful in fooling a classification system, $\mathcal{F}()$, when an input sample \mathbf{x} can be perturbed by a small amount δ to cause a change in the output class,

$$\mathcal{F}(\mathbf{x}) \neq \mathcal{F}(\mathbf{x} + \delta). \quad (1)$$

It is necessary for adversarial attacks to be *imperceptible*, such that adversarial perturbations are not easily detectable/noticeable by humans. For images, an imperceptibility constraint is usually enforced using the l_p norm, with $p = \infty$ being the most popular choice, as a proxy to measure human perception,

$$\|\delta\|_\infty \leq \epsilon, \quad (2)$$

where ϵ is the maximum perturbation size permitted for a change to be deemed appropriately imperceptible. The simplest adversarial attack method for images is Finite Gradient Sign Method (FGSM) [8]. Here, the perturbation direction,

δ , is in the direction of the largest gradient of the output loss function, $\mathcal{L}()$, for a model with parameters θ ,

$$\delta = \epsilon \text{sign}(\nabla_{\mathbf{x}} \mathcal{L}(\theta, \mathbf{x}, y)), \quad (3)$$

where the `sign()` functions returns $+1$ or -1 , element-wise and y is the target class (or the original predicted class by the model). The Basic Iterative Method (BIM) [18] improves upon the FGSM method, but the most powerful first order image attack method is generally Project Gradient Descent (PGD) [20]. The PGD method adapts the iterative process of BIM to include random initialization and projection. Specifically, an adversarial example \mathbf{x}'_0 is initialized randomly by selecting a point uniformly on the l_∞ ball around \mathbf{x} . Then this adversarial example is updated iteratively,

$$\mathbf{x}'_{i+1} = \prod_{\mathbf{x} \in \mathcal{S}} [\mathbf{x}'_i + \alpha \text{sign}(\nabla_{\mathbf{x}} \mathcal{L}(\theta, \mathbf{x}, y))|_{\mathbf{x}=\mathbf{x}'_i}], \quad (4)$$

where \prod denotes the projection operator for mapping back into the space of all acceptable perturbations \mathcal{S} around \mathbf{x} (element-wise clipping to ensure the elements are within the l_∞ ball of size ϵ around \mathbf{x}) and α is a tunable gradient step. The PGD attack can be run for t iterations. The adversarial perturbation, δ is then simply $\delta = \mathbf{x}'_t - \mathbf{x}$.

4. Sample Attackability

Sample attackability aims to understand, *how easy is it* to attack a specific sample. For a specific model, \mathcal{F}_k , we can state a sample, n 's attackability can be measured directly by the smallest perturbation required to change the classification of the model,

$$\hat{\delta}_n^{(k)} = \min_{\delta} (\mathcal{F}_k(\mathbf{x}_n) \neq \mathcal{F}_k(\mathbf{x}_n + \delta)). \quad (5)$$

A successful adversarial attack requires the perturbation to be imperceptible, as measured by the proxy function in Equation 2. However, as this is only a proxy measure and there exists variation in what humans deem imperceptible, it is difficult to decide on a single value for ϵ in the imperceptibility constraint. Hence, in this work, we define sample n as *attackable* for model k if the magnitude of the optimal adversarial perturbation is less than a strict threshold, $\mathbf{A}_{n,k} = (|\hat{\delta}_n^{(k)}| < \epsilon_a)$, where any sample that is not attackable can be denoted as $\bar{\mathbf{A}}_{n,k}$. Conversely, a sample is defined as *robust*, if its adversarial perturbation size is larger than a separate, but more generous (larger) set threshold, $\mathbf{R}_{n,k} = (|\hat{\delta}_n^{(k)}| > \epsilon_r)$.

However, it is useful to identify samples that are *universally* attackable/robust, i.e. the definition is agnostic to a specific model architecture or model realisation, k , used. We can thus extend the definition for *universality* as follows. A sample, n , is **universally attackable** if,

$$\mathbf{A}_n^{(\mathcal{M})} = \bigcap_{k, \mathcal{F}_k \in \mathcal{M}} \mathbf{A}_{n,k}, \quad (6)$$

where \mathcal{M} is the set of models in consideration. Similarly a sample is **universally robust** if, $\mathbf{R}_n^{(\mathcal{M})} = \bigcap_{k, \mathcal{F}_k \in \mathcal{M}} \mathbf{R}_{n,k}$. The definition of attackability does not explicitly consider the adversarial attack method used to determine the adversarial perturbations. Experiments in Section 6 demonstrate that the rank correlation of samples between different attack methods (FGSM and PGD) is extremely high, suggesting that only the thresholds ϵ_a and ϵ_r have to be adjusted to ensure the same samples are defined as attackable or robust, independent of the attack method used.

5. Attackable and Robust Sample Detection

Section 4 defines attackable ($\mathbf{A}_{n,k}$) and robust ($\mathbf{R}_{n,k}$) samples. This section introduces a deep-learning based method to identify the attackable and robust samples in an unseen dataset, for an unseen target model, \mathcal{F}_t . Let the deep-learning attackability detector have access to a seen dataset, $\{\mathbf{x}_n, y_n\}_{n=1}^N$ and a set of seen models, $\mathcal{M} = \{\mathcal{F}_1, \dots, \mathcal{F}_{|\mathcal{M}|}\}$, such that $\mathcal{F}_t \notin \mathcal{M}$. Each model can be represented as an encoding stage, followed by a classification stage,

$$\mathcal{F}_k(\mathbf{x}_n) = \mathcal{F}_k^{(c1)}(\mathbf{h}_{n,k}), \quad (7)$$

where $\mathbf{h}_{n,k}$ is the output of the model's encoding of \mathbf{x}_n . A separate attackability detector can be trained for each seen model in \mathcal{M} . For a specific seen model, k , we can measure the attackability of each sample using the minimum perturbation size (Equation 5), $\{\hat{\delta}_n^{(k)}\}_{n=1}^N$. It is useful and efficient to exploit the encoding representation of input images, $\mathbf{h}_{n,k}$, already learnt by each model. Hence, each deep attackability detector, $\mathcal{D}_\theta^{(k)}$, with parameters θ , can be trained as a binary classification task to determine the probability of a sample being attackable for model k , using the encoding at the input,

$$p(\mathbf{A}_{n,k}) = \mathcal{D}_\theta^{(k)}(\mathbf{h}_{n,k}). \quad (8)$$

This work uses a simple, single hidden-layer fully connected network architecture for each detector, \mathcal{D} , such that,

$$\mathcal{D}_\theta(\mathbf{h}) = \sigma(\mathbf{W}_1 \sigma(\mathbf{W}_0 \mathbf{h})), \quad (9)$$

where \mathbf{W}_0 and \mathbf{W}_1 are the trainable parameters and $\sigma()$ is a standard sigmoid function. Now, we have a collection model-specific detectors that we want to use to determine the probability of a sample being attackable for the unseen target model, \mathcal{F}_t . The best estimate is to use an average over the model-specific detector attackability probabilities,

$$p(\mathbf{A}_{n,t}) \approx \frac{1}{|\mathcal{M}|} \sum_{k, \mathcal{F}_k \in \mathcal{M}} p(\mathbf{A}_{n,k}). \quad (10)$$

However, it is unlikely that this estimate can capture the samples that are attackable specifically for the target

model, \mathcal{F}_t 's particular architecture and its specific realisation. Hence, instead it is more interesting to estimate the probability of a *universally attackable* sample (defined in Equation 6),

$$p(\mathbf{A}_n^{(\mathcal{M}+t)}) \approx \left[\frac{1}{|\mathcal{M}|} \sum_{k, \mathcal{F}_k \in \mathcal{M}} p(\mathbf{A}_{n,k}) \right]^{\alpha(\mathcal{M})}, \quad (11)$$

where the parameter $\alpha(\mathcal{M})$ models the idea that the probability of sample being universally attackable should decrease with the number of models, i.e. by definition, the number of samples defined as *universally attackable* can only decrease as number of models in \mathcal{M} increases, as is observed in Figure 1 with the *uni* curve lying below all the model-specific curves. Hence, $\alpha(\mathcal{M}) \geq 1$ and increases with $|\mathcal{M}|$ ².

Similarly, detectors can be trained to determine the probability of a sample being universally robust, $p(\mathbf{R}_n^{(\mathcal{M}+t)})$. As a simpler alternative to a deep attackability detector, uncertainty-based detectors can also be used to identify attackable/robust samples. The simplest form of uncertainty is negative confidence (probability of the predicted class), where it is intuitively expected that the most confident predictions will be for the *robust* samples, $\text{conf}_k(\mathbf{x}) > \rho_r$ and the least confidence samples can be classed as *attackable*, $\text{conf}_k(\mathbf{x}) < \rho_a$.

We can evaluate the performance of the attackability detectors on the unseen target model, $\mathcal{F}_t \notin \mathcal{M}$, using four variations on defining a sample, n as attackable:

1. **all** - the sample is attackable for the unseen target model.

$$\mathbf{A}_{n,t} = (|\hat{\delta}_n^{(t)}| < \epsilon_a). \quad (12)$$

2. **uni** - the sample is universally attackable for the unseen models and the target model.

$$\mathbf{A}_n^{(\mathcal{M}+t)} = \mathbf{A}_{n,t} \cap \mathbf{A}_n^{(\mathcal{M})}. \quad (13)$$

3. **spec** - the sample is attackable for the target model but not universally attackable for the seen models.

$$\mathbf{A}_{n,t}^{\text{spec}} = \mathbf{A}_{n,t} \cap \bar{\mathbf{A}}_n^{(\mathcal{M})}. \quad (14)$$

4. **vspec** - a sample is specifically attackable for the unseen target model only.

$$\mathbf{A}_{n,t}^{\text{vspec}} = \mathbf{A}_{n,t} \cap \left(\bigcap_{k, \mathcal{F}_k \in \mathcal{M}} \bar{\mathbf{A}}_{n,k} \right). \quad (15)$$

²An alternative product-based model for universal attackability was considered: $p(\mathbf{A}_n^{(\mathcal{M}+t)}) \approx \left[\prod_{k, \mathcal{F}_k \in \mathcal{M}} p(\mathbf{A}_{n,k}) \right]^{\alpha(\mathcal{M})}$, but empirical results with this method were slightly worse for attackable and robust sample detection.

As discussed for Equation 11, it is expected that the deep learning-based detectors will perform best in the **uni** evaluation setting.

For an unseen dataset, we can evaluate the performance of attackability detectors using precision and recall. We select a specific threshold, β , used to class the output of detectors, e.g. $p(\mathbf{A}_n^{(\mathcal{M}+t)}) > \beta$ classes sample n as attackable. The precision is $\text{prec} = \text{TP}/(\text{TP}+\text{FP})$ and recall is $\text{rec} = \text{TP}/(\text{TP}+\text{FN})$, where FP , TP and FN are standard counts for False-Positive, True-Positive and False-Negative. A single value summary is given using the F1-score, $\text{F1} = 2 * (\text{prec} * \text{rec})/(\text{prec} + \text{rec})$. We can generate a full precision-recall curve by sweeping over all thresholds, β and then select the best F1 score.

6. Experiments

6.1. Experimental Setup

Attackability detection experiments are carried out on two standard classification benchmark datasets: Cifar10 and Cifar100 [17]. Cifar10 consists of 50,000 training images and 10,000 test images, uniformly distributed over 10 image classes. Cifar100 is a more challenging dataset, with the same number of train/test images, but distributed over 100 different classes. For both datasets, the training images were randomly separated into a *train* and *validation* set, using a 80-20% split ratio. For training the attackability detectors, direct access was provided to only the validation data and the test data is used to assess the performance.

Four state of the art different model architectures are considered. Model performances are given in Table 1³. Three models (vgg, resnext and densenet) are treated as *seen* models, \mathcal{M} , that the attackability detector has access to during training. The wide-resnet (wrn) model is maintained as an *unseen* model, $\mathcal{F}_t \notin \mathcal{M}$ used only to assess the performance of the attackability detector, as described in Section 5.

Model	Cifar10	Cifar100
vgg-19	93.3	71.8
resnext-29-8-64	96.2	82.5
densenet-121/190-40	87.5	82.7
wrn-28-10	96.2	81.6

Table 1. Model Accuracy (%)

Two adversarial attack types are considered in these experiments: FGSM (Equation 3) and the PGD (Equation 4). The FGSM attack is treated as a *known* attack type, which

³Saved model parameters, hyper-parameter training details and code for all models is provided as a public repository: <https://github.com/bearpaw/pytorch-classification>

the attackability detector has knowledge of during training, whilst the more powerful PGD attack is an *unknown* attack type, reserved for evaluation of the detector. In summary, these experiments use three *seen* models, the validation set and FGSM-based attacks to train an attackability detector. This detector is then required to identify robust/attackable samples for an unseen test set and an unseen target model, attacked using either the known FGSM (*matched* evaluation) or PGD (*unmatched* evaluation).

6.2. Results

Initial experiments consider the *matched* evaluation setting. For each *seen* model (vgg, resnext and densenet), the FGSM method is used to determine the minimum perturbation size, $\hat{\delta}_n^{(k)}$, required to successfully attack each sample, n in the validation dataset for model k (Equation 5). Figure 1 shows (for Cifar100 as an example) the fraction, f of samples that are successfully attacked for each model, as the adversarial attack constraint, ϵ_a is varied: $f = \frac{1}{N} \sum_n \mathbb{1}_{A_{n,k}}$. Based on this distribution, any samples with a perturbation size below $\epsilon_a = 0.05$ are termed *attackable* and any samples with a perturbation size above $\epsilon_r = 0.39$ are termed *robust*. Note that the *uni* curve in Figure 1 shows the fraction of *universally* attackable samples, i.e. these samples are attackable as per all three models (Equation 6).

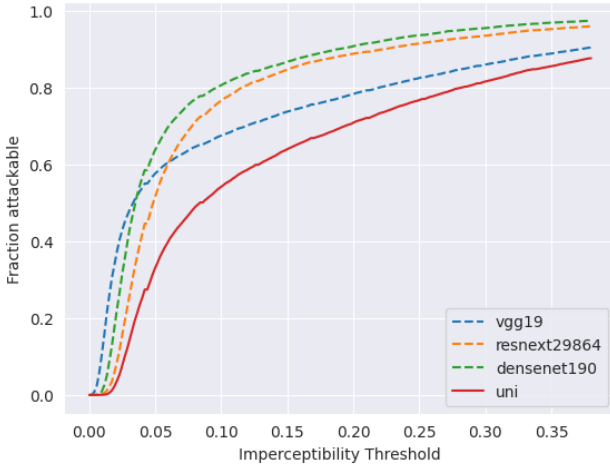


Figure 1. Fraction of *attackable* samples.

Section 5 describes a simple method to train a deep learning classifier to detect robust/attackable samples. Hence, a single layer fully connected network (Equation 9) is trained with *seen* (vgg, resnext, densenet) model’s encodings⁴, using the validation samples in two binary classification settings: 1) detect attackable samples and 2) detect robust sam-

⁴Encoding stage for each model defined in: https://github.com/rainavyas/img_attackability/blob/main/src/models/model_embedding.py

ples. The number of hidden layer nodes for each model’s FCN is set to the encoder output size. Training of the FCNs used a batch-size of 64, 200 epochs, a learning rate of 1e-3 (with a factor 10 drop at epochs 100 and 150), momentum of 0.9 and weight decay of 1e-4 with stochastic gradient descent. As described in Section 5, an ensemble of the confidence of the three seen architectures (conf-s) and the confidence of the unseen architecture, wrn, (conf-u) are also used as uncertainty based detectors for comparison to the deep-learning based (deep) attackability/robust sample detector. To better understand the operation of the detectors, Section 5 defines four evaluation settings: all (Equation 12), uni (Equation 13), spec (Equation 14) and vspec (Equation 15). Table 2 shows the F1 scores for detecting *attackable* samples on the unseen test data for the unseen wrn model, in the matched setting (FGSM attack used to define perturbation sizes for each sample in the test dataset). Note that the scale of F1 scores can vary significantly between evaluation settings as the prevalence of samples defined as *attackable* in a dataset are different for each setting. Table 3 presents the equivalent results for detecting robust samples, where the definitions for each evaluation setting update to identifying *robust* samples ($R_{n,k}$). For Cifar10 data, the deep unseen detection method performs the best only in the *uni* evaluation setting for both attackable and robust sample detection. This is perhaps expected due to the deep detection method having been designed for this purpose (Equation 11), whilst for example the *conf seen* detection method has direct access to the target unseen model (wrn) and is able to perform better in the *spec* and *vspec* settings. When evaluation is on *all* attackable/robust samples for wrn, the superior *vspec* and *spec* performances of the uncertainty detectors, allows them to do better overall. However, for Cifar100 data, the deep detection method is able to perform significantly better in every setting other than the *vspec* evaluation setting, which is expected as this detector has no access to the target model and cannot identify samples specifically attackable/robust for the target model (wrn).

Setting		conf-s	conf-u	deep
all	cifar10	0.693	0.681	0.683
	cifar100	0.845	0.851	0.874
uni	cifar10	0.660	0.643	0.682
	cifar100	0.792	0.827	0.831
spec	cifar10	0.239	0.209	0.206
	cifar100	0.263	0.261	0.271
vspec	cifar10	0.010	0.006	0.006
	cifar100	0.018	0.018	0.018

Table 2. Attackable Sample Detection (F1) in matched setting.

Figure 2(a-b) presents the full precision-recall curves (as

Setting		conf-s	conf-u	deep
all	cifar10	0.501	0.502	0.435
	cifar100	0.134	0.161	0.385
uni	cifar10	0.030	0.090	0.251
	cifar100	0.026	0.074	0.565
spec	cifar10	0.486	0.485	0.422
	cifar100	0.119	0.141	0.286
vspec	cifar10	0.300	0.288	0.254
	cifar100	0.042	0.061	0.055

Table 3. Robust Sample Detection in matched setting.

described in Section 5) for detecting robust samples in the *uni* evaluation setting, which the deep-learning based detector has been designed for. It is evident that for a large range of operating points, the deep detection method dominates and is thus truly a useful method for identifying robust samples. Figure 2(c-d) presents the equivalent precision-recall curves for detecting attackable samples. Here, although the deep-learning method still dominates over the uncertainty-based detectors, the differences are less significant. Hence, it can be argued that this deep learning-based attackability detector is capable of identifying both attackable and robust samples, but is particularly powerful in detecting robust samples.

In the unmatched evaluation setting the aim is to identify the attackable/robust samples in the test data, where the perturbation sizes for each sample are calculated using the more powerful *unknown* PGD attack method (Equation 4). PGD attacks used 8 iterations of the attack loop. For each model and dataset, the known FGSM attack and the unknown PGD attacks were used to rank samples in the validation set by the perturbation size, $|\delta_n|$. In all cases the Spearman Rank correlation is greater than 0.84 for Cifar10 and 0.90 for Cifar100 (Table 4). This implies that the results from the matched setting should transfer easily to the unmatched setting. Table 5 gives the F1 scores for detecting

	vgg	resnext	densenet
cifar10	0.840	0.849	0.951
cifar100	0.947	0.900	0.911

Table 4. Spearman rank correlation (PGD, FGSM) perturbations.

universal attackable/robust samples in the unmatched setting. As the PGD attack is more powerful than the FGSM attack, the definition of the attackable threshold and robustness threshold are adjusted to $\epsilon_a = 0.03$ and $\epsilon_r = 0.10$. The deep unseen detectors dominate once again (specifically for robust sample detection) and thus, the trends identified for the matched evaluation setting are maintained in the more

challenging unmatched setting.

Uni setting		conf-s	conf-u	deep
Attackable	cifar10	0.636	0.754	0.777
	cifar100	0.846	0.871	0.893
Robust	cifar10	0.008	0.008	0.048
	cifar100	0.005	0.006	0.233

Table 5. Attackable/Robust sample detection (unmatched setting).

Active Adversarial Training: Adversarial training [23] is performed by further training trained models on adversarial examples, generated by adversarially attacking original data samples. However, it is computationally expensive to adversarially attack every original data sample. Hence, it is useful to *actively* select a subset of the most *useful* samples for adversarial training. Active adversarial training can be viewed as a strict form of weighted adversarial training [12], where adversarial examples are re-weighed in importance during training. Figure 3 shows the robustness (measured by fooling rate)⁵ of the target wide-resnet model when adversarially trained using adversarial examples from a subset of the Cifar10 validation data, where the subset is created by different ranking methods: random; a popular *entropy-aware* approach [16], where ranking is as per the uncertainty (entropy) of the trained wide-resnet model (uncertainty); and the final ranking method uses the attackability of original validation samples as per the deep attackability detector from this work. The adversarially trained model’s robustness is evaluated using the fooling rate on the test Cifar10 data. It is evident that the deep attackability detector gives the most robust model for any fraction of data used for adversarial training. Specifically, with this detector, only 40% of the samples have to be adversarially attacked for adversarial training to give competitive robustness gains.

7. Conclusion

This work proposes a novel perspective on adversarial attacks by introducing the concept of sample attackability and robustness. A sample can be defined as attackable if its minimum perturbation size (for a successful adversarial attack) is less than a set threshold and conversely a sample can be defined as robust if its minimum perturbation size is greater than another set threshold. A deep-learning based attackability detector is trained to identify universally attackable/robust samples for unseen data and an unseen target model. In comparison to uncertainty-based attackability detectors, the deep-learning method performs best, with significant gains for robust sample detection. The understanding of sample attackability and robustness can have

⁵Robustness evaluated on test data attacked using PGD, with $\epsilon = 0.03$.

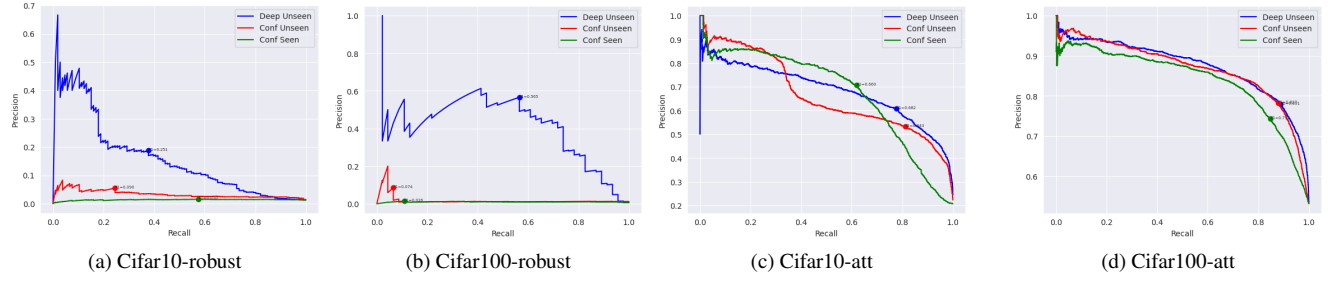


Figure 2. P-R curves for detecting *universal* robust/attackable samples.

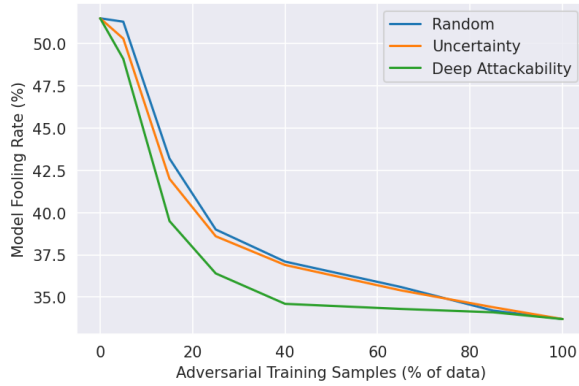


Figure 3. Active Adversarial Training

important implications for various tasks such as active adversarial training. Future work can explore the significance of attackability on the design of more robust systems.

References

- [1] Tao Bai, Jingqi Luo, Jun Zhao, Bihan Wen, and Qian Wang. Recent advances in adversarial training for adversarial robustness. In Zhi-Hua Zhou, editor, *Proceedings of the Thirtieth International Joint Conference on Artificial Intelligence, IJCAI-21*, pages 4312–4321. International Joint Conferences on Artificial Intelligence Organization, 8 2021. Survey Track. [1](#)
- [2] Battista Biggio and Fabio Roli. Wild patterns: Ten years after the rise of adversarial machine learning. *CoRR*, abs/1712.03141, 2017. [1](#)
- [3] Anirban Chakraborty, Manaar Alam, Vishal Dey, Anupam Chattopadhyay, and Debdeep Mukhopadhyay. Adversarial attacks and defences: A survey. *CoRR*, abs/1810.00069, 2018. [1](#)
- [4] Melanie Ducoffe and Frédéric Precioso. Adversarial active learning for deep networks: a margin based approach. *CoRR*, abs/1802.09841, 2018. [1](#)
- [5] Jakob Gawlikowski, Cedrique Rovile Njieutcheu Tassi, Mohsin Ali, Jongseok Lee, Matthias Humt, Jianxiang Feng, Anna M. Kruspe, Rudolph Triebel, Peter Jung, Ribana Roscher, Muhammad Shahzad, Wen Yang, Richard Bamler, and Xiao Xiang Zhu. A survey of uncertainty in deep neural networks. *CoRR*, abs/2107.03342, 2021. [2](#)
- [6] Partha Ghosh, Arpan Losalka, and Michael J. Black. Resisting adversarial attacks using gaussian mixture variational autoencoders. *CoRR*, abs/1806.00081, 2018. [2](#)
- [7] Justin Gilmer, Luke Metz, Fartash Faghri, Samuel S. Schoenholz, Maithra Raghu, Martin Wattenberg, and Ian J. Goodfellow. Adversarial spheres. *CoRR*, abs/1801.02774, 2018. [2](#)
- [8] Ian J. Goodfellow, Jonathon Shlens, and Christian Szegedy. Explaining and harnessing adversarial examples, 2014. [1, 2](#)
- [9] Shixiang Gu and Luca Rigazio. Towards deep neural network architectures robust to adversarial examples, 2014. [2](#)
- [10] Zhengyu He. Deep learning in image classification: A survey report. In *2020 2nd International Conference on Information Technology and Computer Application (ITCA)*, pages 174–177, 2020. [1](#)
- [11] Dan Hendrycks and Kevin Gimpel. Visible progress on adversarial images and a new saliency map. *CoRR*, abs/1608.00530, 2016. [1](#)
- [12] Chester Holtz, Tsui-Wei Weng, and Gal Mishne. Learning sample reweighting for accuracy and adversarial robustness, 2022. [1, 2, 6](#)
- [13] Ngoc Dung Huynh, Mohamed Reda Bouadjenek, Imran Razzaq, Kevin Lee, Chetan Arora, Ali Hassani, and Arkady Zaslavsky. Adversarial attacks on speech recognition systems for mission-critical applications: A survey, 2022. [1](#)
- [14] Rauf Izmailov, Shridatt Sugrim, Ritu Chadha, Patrick McDaniel, and Ananthram Swami. Enablers of adversarial attacks in machine learning. In *MILCOM 2018 - 2018 IEEE Military Communications Conference (MILCOM)*, pages 425–430, 2018. [2](#)
- [15] Diksha Khurana, Aditya Koli, Kiran Khatter, and Sukhdev Singh. Natural language processing: State of the art, current trends and challenges. *CoRR*, abs/1708.05148, 2017. [1](#)
- [16] Minseong Kim, Jihoon Tack, Jinwoo Shin, and Sung Ju Hwang. Entropy weighted adversarial training. 2021. [2, 6](#)
- [17] Alex Krizhevsky. Learning multiple layers of features from tiny images. pages 32–33, 2009. [4](#)
- [18] Alexey Kurakin, Ian J. Goodfellow, and Samy Bengio. Adversarial machine learning at scale. *CoRR*, abs/1611.01236, 2016. [3](#)
- [19] Hyungill Lee, Sungyeob Han, and Jungwoo Lee. Generative adversarial trainer: Defense to adversarial perturbations with GAN. *CoRR*, abs/1705.03387, 2017. [2](#)
- [20] Aleksander Madry, Aleksandar Makelov, Ludwig Schmidt, Dimitris Tsipras, and Adrian Vladu. Towards deep learning models resistant to adversarial attacks, 2017. [2, 3](#)
- [21] Dongyu Meng and Hao Chen. Magnet: a two-pronged defense against adversarial examples. *CoRR*, abs/1705.09064, 2017. [2](#)
- [22] Awais Muhammad and Sung-Ho Bae. A survey on efficient methods for adversarial robustness. *IEEE Access*, 10:118815–118830, 2022. [1](#)
- [23] Zhuang Qian, Kaizhu Huang, Qiu-Feng Wang, and Xu-Yao Zhang. A survey of robust adversarial training in pattern recognition: Fundamental, theory, and methodologies, 2022. [1, 2, 6](#)
- [24] Vyas Raina and Mark Gales. Residue-based natural language adversarial attack detection. In *Proceedings of the 2022 Conference of the North American Chapter of the Association for Computational Linguistics: Human Language Technologies*. Association for Computational Linguistics, 2022. [1](#)
- [25] Pengzhen Ren, Yun Xiao, Xiaojun Chang, Po-Yao Huang, Zhihui Li, Xiaojiang Chen, and Xin Wang. A survey of deep active learning. *CoRR*, abs/2009.00236, 2020. [1, 2](#)
- [26] Dongyu Ru, Jiangtao Feng, Lin Qiu, Hao Zhou, Mingxuan Wang, Weinan Zhang, Yong Yu, and Lei Li. Active sentence learning by adversarial uncertainty sampling in discrete space. In *Findings of the Association for Computational Linguistics: EMNLP 2020*, pages 4908–4917, Online, Nov. 2020. Association for Computational Linguistics. [1](#)
- [27] Ayon Sen, Xiaojin Zhu, Erin Marshall, and Robert Nowak. Popular imperceptibility measures in visual adversarial attacks are far from human perception. In Quanyan Zhu, John S. Baras, Radha Poovendran, and Juntao Chen, editors, *Decision and Game Theory for Security*, pages 188–199, Cham, 2020. Springer International Publishing. [1](#)
- [28] Alex Serban, Erik Poll, and Joost Visser. Adversarial examples on object recognition: A comprehensive survey. *CoRR*, abs/2008.04094, 2020. [1](#)
- [29] Uri Shaham, James Garritano, Yutaro Yamada, Ethan Weinberger, Alex Cloninger, Xiuyuan Cheng, Kelly Stanton, and Yuval Kluger. Defending against adversarial images using basis functions transformations, 2018. [1](#)
- [30] Chaomin Shen, Yixin Peng, Guixu Zhang, and Jinsong Fan. Defending against adversarial attacks by suppressing the largest eigenvalue of fisher information matrix. *CoRR*, abs/1909.06137, 2019. [1](#)
- [31] Lewis Smith and Yarin Gal. Understanding measures of uncertainty for adversarial example detection, 2018. [1](#)

- [32] Yang Song, Taesup Kim, Sebastian Nowozin, Stefano Ermon, and Nate Kushman. Pixeldefend: Leveraging generative models to understand and defend against adversarial examples. *CoRR*, abs/1710.10766, 2017. [2](#)
- [33] Li-Li Sun and Xi-Zhao Wang. A survey on active learning strategy. In *2010 International Conference on Machine Learning and Cybernetics*, volume 1, pages 161–166, 2010. [1, 2](#)
- [34] Christian Szegedy, Wojciech Zaremba, Ilya Sutskever, Joan Bruna, Dumitru Erhan, Ian Goodfellow, and Rob Fergus. Intriguing properties of neural networks, 2013. [2](#)
- [35] Thomas Tanay and Lewis D. Griffin. A boundary tilting perspective on the phenomenon of adversarial examples. *CoRR*, abs/1608.07690, 2016. [2](#)
- [36] Jianhan Xu, Cenyuan Zhang, Xiaoqing Zheng, Linyang Li, Cho-Jui Hsieh, Kai-Wei Chang, and Xuanjing Huang. Towards adversarially robust text classifiers by learning to reweight clean examples. In *Findings of the Association for Computational Linguistics: ACL 2022*, pages 1694–1707, Dublin, Ireland, May 2022. Association for Computational Linguistics. [2](#)
- [37] Huimin Zeng, Chen Zhu, Tom Goldstein, and Furong Huang. Are adversarial examples created equal? A learnable weighted minimax risk for robustness under non-uniform attacks. *CoRR*, abs/2010.12989, 2020. [2](#)
- [38] Wei Emma Zhang, Quan Z. Sheng, and Ahoud Alhazmi. Generating textual adversarial examples for deep learning models: A survey. *CoRR*, abs/1901.06796, 2019. [1](#)